

RESEARCH ARTICLE

Open Access



Boron-deficiency-responsive microRNAs and their targets in *Citrus sinensis* leaves

Yi-Bin Lu^{1,2}, Yi-Ping Qi³, Lin-Tong Yang^{1,2}, Peng Guo^{1,2}, Yan Li¹ and Li-Song Chen^{1,2,4,5*}

Abstract

Background: MicroRNAs play important roles in the adaptive responses of plants to nutrient deficiencies. Most research, however, has focused on nitrogen (N), phosphorus (P), sulfur (S), copper (Cu) and iron (Fe) deficiencies, limited data are available on the differential expression of miRNAs and their target genes in response to deficiencies of other nutrient elements. In this study, we identified the known and novel miRNAs as well as the boron (B)-deficiency-responsive miRNAs from citrus leaves in order to obtain the potential miRNAs related to the tolerance of citrus to B-deficiency.

Methods: Seedlings of 'Xuegan' [*Citrus sinensis* (L.) Osbeck] were supplied every other day with B-deficient (0 μ M H_3BO_3) or -sufficient (10 μ M H_3BO_3) nutrient solution for 15 weeks. Thereafter, we sequenced two small RNA libraries from B-deficient and -sufficient (control) citrus leaves, respectively, using Illumina sequencing.

Results: Ninety one (83 known and 8 novel) up- and 81 (75 known and 6 novel) down-regulated miRNAs were isolated from B-deficient leaves. The great alteration of miRNA expression might contribute to the tolerance of citrus to B-deficiency. The adaptive responses of miRNAs to B-deficiency might related to several aspects: (a) attenuation of plant growth and development by repressing auxin signaling due to decreased *TIR1* level and ARF-mediated gene expression by altering the expression of *miR393*, *miR160* and *miR3946*; (b) maintaining leaf phenotype and enhancing the stress tolerance by up-regulating *NACs* targeted by *miR159*, *miR782*, *miR3946* and *miR7539*; (c) activation of the stress responses and antioxidant system through down-regulating the expression of *miR164*, *miR6260*, *miR5929*, *miR6214*, *miR3946* and *miR3446*; (d) decreasing the expression of *major facilitator superfamily protein genes* targeted by *miR5037*, thus lowering B export from plants. Also, B-deficiency-induced down-regulation of *miR408* might play a role in plant tolerance to B-deficiency by regulating Cu homeostasis and enhancing superoxide dismutase activity.

Conclusions: Our study reveals some novel responses of citrus to B-deficiency, which increase our understanding of the adaptive mechanisms of citrus to B-deficiency at the miRNA (post-transcriptional) level.

Keywords: Boron-deficiency, *Citrus sinensis*, Illumina sequencing, Leaves, MicroRNA

Background

Boron (B), an essential micronutrient for normal growth and development of plants, is involved in a series of important physiological functions, including the structure of cell walls, membrane integrity, cell division, phenol metabolism, protein metabolism and nucleic acid metabolism during growth and development of higher plants [1–5]. B-deficiency widespreadly exists in many

agricultural crops, including citrus. In China, B-deficiency is frequently observed in citrus orchards, and often contributes to the loss of productivity and poor fruit quality [3]. Li et al. reported that up to 9.0 % and 43.5 % of 'Guanximiyou' pummelo (*Citrus grandis*) orchards in Pinghe, Zhangzhou, China were deficient in leaf B and soil water-soluble B, respectively [6].

In plants, approx. 21-nucleotide-long microRNAs (miRNAs), one of the most abundant classes of non-coding small RNAs (sRNAs), are crucial post-transcriptional regulators of gene expression by repressing translation or directly degrading mRNAs in plants [7]. Evidence shows that miRNAs play key roles in plant response to nutrient

* Correspondence: lisongchen2002@hotmail.com

¹College of Resource and Environmental Science, Fujian Agriculture and Forestry University, Fuzhou 350002, China

²Institute of Horticultural Plant Physiology, Biochemistry and Molecular Biology, Fujian Agriculture and Forestry University, Fuzhou 350002, China
Full list of author information is available at the end of the article

deficiencies [8–13]. Identification of nutrient-deficiency-responsive-miRNAs and their target genes has become one of the hottest topics in plant nutrition.

Plants have developed diverse strategies to maintain phosphorus (P) homeostasis, including miRNA regulations [11, 12]. *MiR399*, which is specifically induced by P-deficiency in *Arabidopsis* and rice, can regulate P homeostasis by negatively regulating its target gene *UBC24* [13, 14]. Like *miR399*, *miR827* is also highly and specifically induced by P-deficiency and is involved in the regulation of plant P homeostasis by down-regulating its target gene *nitrogen limitation adaptation (NLA)* in *Arabidopsis* [13]. In addition, many other P-deficiency-responsive miRNAs (i.e., *miR1510*, *miR156*, *miR159*, *miR166*, *miR169*, *miR2109*, *miR395*, *miR397*, *miR398*, *miR408*, *miR447* and *miR482*) have been isolated from various plant species [15–21].

MiR397, *miR398*, *miR408*, and *miR857*, which are induced by copper (Cu)-deficiency, have been shown to play a role in the regulation of Cu homeostasis by down-regulating genes encoding nonessential Cu proteins such as Cu/Zn superoxide dismutase (SOD), laccases and plantacyanin, hence saving Cu for other essential Cu proteins such as plastocyanin, which is essential for photosynthesis [10, 22, 23].

In *Arabidopsis*, leaf *miR395* was induced by sulfur (S)-deficiency. *MiR395* targets *ATP sulfurylases (APS)* and *sulfate transporter 2;1 (SULTR2;1)*, both of which are involved in the S metabolism. Their transcripts are greatly down-regulated in *miR395*-over-expressing transgenic *Arabidopsis* accompanied by increased accumulation of S in the shoot but not in the root. They concluded that *miR395* play a role in the regulation of plant S accumulation and allocation by targeting *APS* and *SULTR2;1* [24].

MiRNAs have been shown to play a role in the adaptation of plants to Fe-deficiency. Eight Fe-deficiency-responsive conserved miRNAs from five families had been identified in *Arabidopsis* roots and shoots and their expression profiles differed between the two organs [25]. Valdés-López et al. isolated ten up- and four down-regulated miRNAs, five up- and six down-regulated miRNAs, and seven up- and four down-regulated miRNAs from the leaves, roots and nodules of Fe-deficient common bean [17]. Waters et al. obtained eight differentially expressed miRNAs from seven conserved families in the rosettes of Fe-deficient *Arabidopsis*. Interestingly, Fe-deficiency led to increased accumulation of Cu in rosettes and decreased expression levels of *miR397a*, *miR398a* and *miR398b/c*, which regulate the mRNA levels of genes encoding Cu-containing proteins, implying a links between Fe-deficiency with Cu homeostasis [26].

Many N-deficiency-responsive miRNAs have been identified from *Arabidopsis*, soybean, maize and common bean. These miRNAs belong to at least 27 conserved

families [10, 17, 27, 28]. In *Arabidopsis*, the expression of *miR169* was inhibited by N-deficiency, while the expression levels of its target genes [i.e., *NFYA2 (Nuclear Factor Y, subunit A2)*, *NFYA3*, *NFYA5* and *NFYA8*] were increased [10, 13, 27, 29]. Transgenic *Arabidopsis* plants over-expressing *miR169a* had less accumulation of N and *NFYA* family members, and were more sensitive to N stress than the wild type, demonstrating a role for *miR169* in the adaptation of plants to N-deficiency [29]. It is worth noting that some N-deficiency-responsive miRNAs (e.g., *miR169*, *miR172*, *miR394*, *miR395*, *miR397*, *miR398*, *miR399*, *miR827*, *miR408* and *miR857*) are also responsive to other nutrient stresses (i.e., B, P, Fe, S and Cu deficiencies) in plants [8, 10], indicating the involvement of miRNA-mediated crosstalk among N, B, P, Fe, S and Cu under N-deficiency.

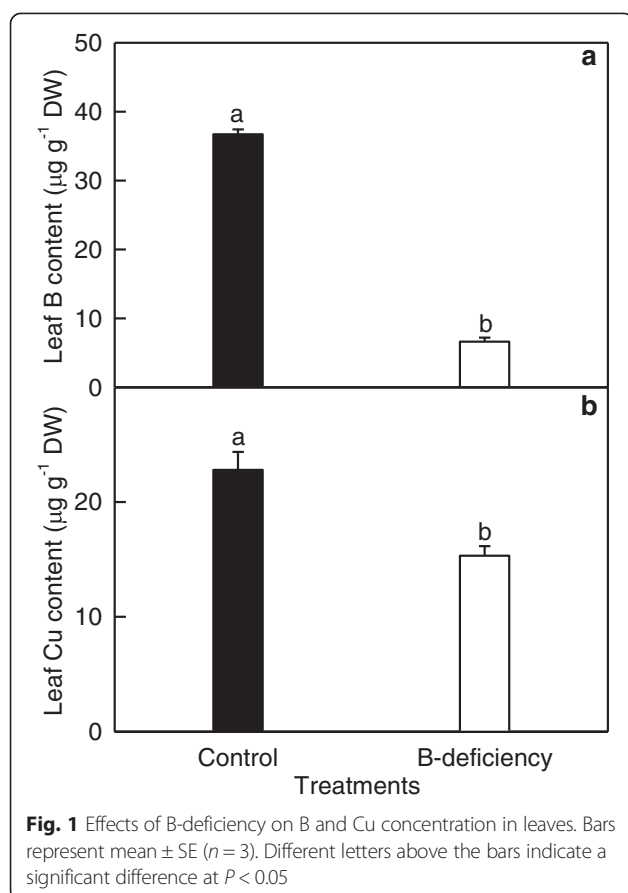
An increasing number of nutrient-deficiency-responsive miRNAs have been identified with different techniques [8–14]. Most research, however, has focused on N, P, S, Cu and Fe deficiencies, limited data are available on the differential expression of miRNAs and their target genes in response to deficiencies of other nutrient elements. Recently, we investigated miRNA expression profiles in response to B-deficiency in *Citrus sinensis* roots by Illumina sequencing and identified 134 (112 known and 22 novel) B-deficiency-responsive miRNAs, suggesting the possible roles of miRNAs in the tolerance of citrus plants to B-deficiency [8]. Previous studies showed that the responses of miRNAs to nutrient deficiencies differed between plant roots and shoots (leaves) [12, 17, 25]. In addition, there were great differences in B-deficiency-induced changes in major metabolites, activities of key enzymes involved in organic acid and amino acid metabolism, gas exchange and gene expression profiles between roots and leaves of *C. sinensis* [4, 30]. Therefore, B-deficiency-induced changes in miRNA expression profiles should be different between citrus roots and leaves.

In this study, we sequenced two small RNA libraries from B-deficient and -sufficient (control) citrus leaves, respectively, using Illumina sequencing, then identified the known and novel miRNAs as well as the B-deficiency-responsive miRNAs. Also, we predicted the target genes of these known and novel B-deficiency-responsive miRNAs and discussed their possible roles in the response to B-deficiency in citrus. The objective of this study is to identify the potential miRNAs related to the tolerance of citrus to B-deficiency.

Results

B and Cu concentrations in leaves

B concentration in 10 μM B-treated leaves was in the sufficient range of 30 to 100 $\mu\text{g g}^{-1}$ DW, while the value in 0 μM B-treated leaves was much less than 30 $\mu\text{g g}^{-1}$ DW (Fig. 1a) [31]. Visible B-deficient symptoms were



observed only in 0 μM B-treated leaves (data not shown). Therefore, seedlings treated with 0 μM B are considered as B-deficient, and those treated with 10 μM B are considered as B-sufficient. B-deficiency decreased leaf concentration of Cu (Fig. 1b).

Sequencing and analysis of two small RNA libraries from B-sufficient and -deficient citrus leaves

As shown in Table 1, 17,996,827 and 18,223,948 raw reads were generated from the libraries of B-sufficient and -deficient leaves, respectively. After removal of the contaminant reads like adaptors and low quality tags, 17,597,008 and 17,829,966 clear reads were obtained from the libraries of B-sufficient and -deficient leaves, comprising 3,673,054 and 4,654,829 unique clear reads, respectively. Among these reads, 11,726,078 clean reads (1,961,407 unique reads) from B-sufficient leaves and 11,372,875 clean reads (2,484,833 unique reads) from B-deficient leaves were mapped to *C. sinensis* genome (JGI version 1.1, http://phytozome.jgi.doe.gov/pz/portal.html#!info?alias=Org_Csinensis) using SOAP [32]. Exon, intron, miRNA, rRNA, repeat regions, snRNA, snoRNA and tRNA reads were annotated, respectively. After removal of these annotated reads, the remained unique reads that were used to predict novel miRNAs for B-sufficient and -deficient leaves were 3,237,407 and 4,179,224 reads, respectively.

Most of the clear sequences were within the range of 19–26 nt, which accounted for 89 % of the total clear reads. Reads with the length of 24 nt were at the most abundant, followed by the reads with the length of 21, 22, 23 and 20 nt (Additional file 1). Overall, the size distribution of sRNAs agrees with the results obtained on roots of

Table 1 Statistical analysis of sRNA sequencing data from B-sufficient and -deficient leaves of *Citrus sinensis*

	B-sufficiency		B-deficiency	
	Unique sRNAs	Total sRNAs	Unique sRNAs	Total sRNAs
Raw reads		17,996,827		18,223,948
Clear reads	3,673,054 (100 %)	17,597,008 (100 %)	4,654,829 (100 %)	17,829,966 (100 %)
Mapped to genomic	1,961,407 (53.40 %)	11,726,078 (66.64 %)	2,484,833 (53.38 %)	11,372,875 (63.79 %)
Exon antisense	28,626 (0.78 %)	134,009 (0.76 %)	42,754 (0.92 %)	157,929 (0.89 %)
Exon sense	77,868 (2.12 %)	281,505 (1.60 %)	81,887 (1.76 %)	287,483 (1.61 %)
Intron antisense	36,541 (0.99 %)	244,148 (1.39 %)	46,940 (1.01 %)	248,094 (1.39 %)
Intron sense	56,020 (1.53 %)	526,848 (2.99 %)	67,594 (1.45 %)	457,839 (2.57 %)
miRNA	44,496 (1.21 %)	3,858,007 (21.92 %)	46,800 (1.01 %)	2,639,999 (14.81 %)
rRNA	164,311 (4.47 %)	3,052,914 (17.35 %)	158,009 (3.39 %)	2,851,216 (15.99 %)
repeat	821 (0.02 %)	2009 (0.01 %)	1014 (0.02 %)	2718 (0.02 %)
snRNA	2420 (0.07 %)	8040 (0.05 %)	3547 (0.08 %)	10,269 (0.06 %)
snoRNA	1167 (0.03 %)	3628 (0.02 %)	1270 (0.03 %)	4748 (0.03 %)
tRNA	23,377 (0.64 %)	810,902 (4.61 %)	25,790 (0.55 %)	722,780 (4.05 %)
Unannotated sRNAs	3,237,407 (88.14 %)	8,674,998 (49.30 %)	4,179,224 (89.78 %)	10,446,891 (58.59 %)

Citrus sinensis [8], fruits of *C. sinensis* [33] and *Citrus trifoliata*, and flowers of *C. trifoliata* [34]. This indicates that the data of sRNA libraries obtained by the Illumina sequencing are reliable.

Identification of known and novel miRNAs in citrus leaves

Here, a total of 734 known miRNAs were isolated from the two libraries (Additional file 2). The count of reads was normalized to transcript per million (TPM) in order to compare the abundance of miRNAs in the two libraries. The most abundant miRNA isolated from B-sufficient and -deficient libraries was miR157 (86,829.4201 and 48,091.4546 TPM, respectively), followed by miR166 (36,979.7525 and 26148.2271 TPM, respectively) and miR167 (24,944.5815 and 16,269.745, respectively). In this study, only these known miRNAs with normalized read-count more than ten TPM in B-sufficient and/or -deficient leaf libraries were used for further analysis in order to avoid false results caused by the use of low expressed miRNAs [8, 35]. After removal of these low expressed miRNAs, the remained 321 known miRNAs were used for further analysis (Additional file 3).

After removal of these annotated reads (i.e., exon, intron, miRNA, rRNA, repeat regions, snRNA, snoRNA and tRNA), the remained 3,237,407 and 4,179,224 reads from B-sufficient and -deficient libraries, respectively were used to predict novel miRNAs using the Mireap (<http://sourceforge.net/projects/mireap/>). Based on the criteria for annotation of plant miRNAs [7, 36], a total of 71 novel miRNAs were isolated from the two libraries (Additional file 4). Like the known miRNAs, novel miRNAs with normalized read-count less than ten TPM were not included in the expression analysis [7, 35]. After excluding these low expressed novel miRNAs, the remained 28 miRNAs were used for further analysis (Additional file 5).

Identification of B-deficiency-responsive miRNAs in citrus leaves

We identified 91 (83 known and 8 novel) up- and 81 (75 known and 6 novel) down-regulated miRNAs from B-deficient leaves. The most pronounced up- and down-regulated known (novel) miRNAs were miR5266 with a fold-change of 16.22 (novel_miR_95 with a fold-change of 17.61) and miR401 with a fold-change of -15.87 (novel_miR_236 with a fold-change of -18.48), respectively (Additional files 3 and 5).

Validation of high-throughput sequencing results by qRT-PCR

We analyzed the expression of 27 known miRNAs using stem-loop qRT-PCR in order to validate the miRNA expression patterns revealed by Illumina sequencing. The expression levels of all these miRNAs except for *miR6214*,

miR5262 and *miR7841* were comparable in magnitude to the expression patterns obtained by Illumina sequencing (Fig. 2). Obviously, the high-throughput sequencing allowed us to identify the differentially expressed miRNAs under B-deficiency.

Identification of targets for differentially expressed miRNAs and GO analysis

In this study, we predicted 489 and 17 target genes from the 70 known and 6 novel differentially expressed miRNAs, respectively (Additional files 6 and 7). GO categories were assigned to all these target genes based on the cellular component, molecular function and biological process. These target genes for the known and novel miRNAs were related to 12 and 3 components, respectively based on the cellular component. The most three GO terms for known miRNAs were membrane, chloroplast and plastid, while more than 42 % of the target genes for novel miRNAs belonged to membrane (Fig. 3a). Based on the molecular function, the target genes for the known and novel miRNAs genes were grouped into 11 and 9 categories, respectively, the highest percentage of three categories were nucleic acid binding, metal ion binding and transcription factor activity (Fig. 3b). In the biological process, the target genes were mainly focused on response to stress and developmental process for known miRNAs, and nucleic acid metabolic process, developmental process, response to stress and regulation of transcription for novel miRNAs, respectively (Fig. 3c).

qRT-PCR validation of target genes

To verify the expression of the target genes and how the miRNAs regulate their target genes, 77 genes targeted by 14 down- and 13 up-regulated miRNAs were assayed by qRT-PCR (Table 2). Among the 77 genes, the expression changes of 58 target genes showed a negative correlation with their corresponding miRNAs, implying that miRNAs might play a role in regulating gene expression under B-deficiency by cleaving mRNAs. However, the expression changes of the remained 19 target genes had a positive correlation with their corresponding miRNAs, which might be the results of the interaction of different target genes.

Discussion

Evidence shows that miRNAs are involved in the adaptive regulation of higher plants to nutrient deficiencies [8, 13, 17, 19, 24, 27, 37]. Here, we isolated 91 (83 known and 8 novel) up- and 81 (75 known and 6 novel) down-regulated miRNAs from B-deficient leaves (Additional files 3 and 5), indicating that B-deficiency greatly affected the expression profiles of miRNAs in leaves. The differentially expressed miRNAs isolated from leaves were more than from roots [i.e., 52 (40 known and 12 novel) up- and 82 (72

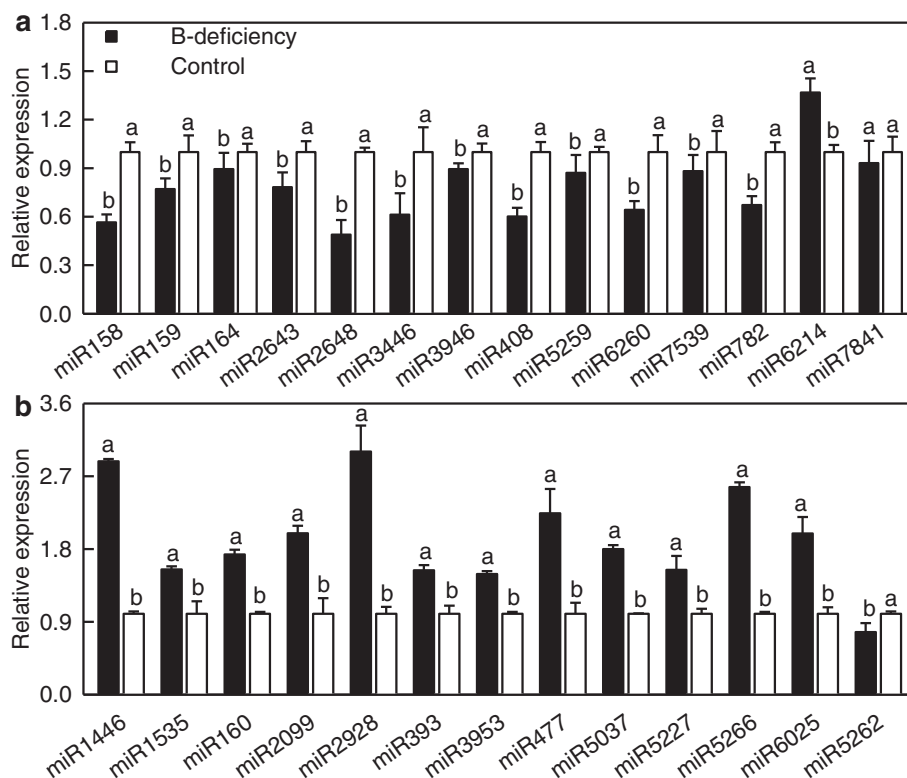


Fig. 2 Relative abundances of selected known miRNAs in B-deficient and control leaves revealed by qRT-PCR. Bars represent mean \pm SD ($n = 3$). Significant differences were tested between control and B-deficient leaves for the same miRNA. Different letters above the bars indicate a significant difference at $P < 0.05$. All the values were expressed relative to the control leaves

known and 10 novel) down-regulated miRNAs] [8]. The majority of the differentially expressed miRNAs were isolated only from B-deficient roots or leaves, only 22 miRNAs were isolated from the both. Moreover, among the 22 miRNAs, 11 miRNAs in roots and leaves displayed different responses to B-deficiency (Table 3). In conclusion, many differences existed in B-deficiency-induced changes in miRNA expression profiles between roots and leaves.

We found that *miR159* was down-regulated in B-deficient leaves (Table 2), as previously obtained on salt stressed sugarcane leaves [38]. Patade and Suprasanna showed that the up-regulation of *MYB* at 1 h of salt-stressed sugarcane leaves was accompanied by the down-regulation of *miR159* [38]. However, the expression of *miR159* was up-regulated in P-deficient soybean (*Glycine max*) roots and leaves [39]. *MiR159* plays important roles in maintaining leaf phenotype by negatively regulating *MYB* transcription factors [40]. Dai et al. reported that the expression of *OsMYB3R-2* was induced by various abiotic stresses, and that over-expression of *OsMYB3R-2* enhanced tolerance to freezing, drought, and salt stress in transgenic *Arabidopsis* [41]. B-1deficiency affects water uptake into the root, transport through the shoot, and loss of water from the leaves [42]. Thus, B-deficiency-induced down-regulation of *miR159* might

increase the expression of *MYBs* (Table 2), thus improving the tolerance of plants to B-deficiency. qRT-PCR showed that all the four *MYBs* target genes (i.e., *MYB domain protein 33*, *MYB domain protein 97*, *MYB-like HTH transcriptional regulator family protein* and *MYB domain protein 65*) were induced by B-deficiency except for the last one. Similarly, the expression levels of *MYB transcription factor (MYBML2)* targeted by *miR782*, *MYB-like HTH transcriptional regulator family protein* and *MYB domain protein 65* targeted by *miR3946*, and *MYB-like HTH transcriptional regulator family protein* and *MYB transcription factor (MYBML2)* targeted by *miR7539* increased in response to B-deficiency except for *MYB domain protein 65* (Table 2). B-deficiency-induced up-regulation of *MYBs* in citrus leaves agrees with the previous report that the expression of *MYB85*, *MYB63* and *MYB42* were up-regulated at the slight corking veins and the seriously corky split veins caused by B-deficiency in 'Newhall' navel orange (*Citrus sinensis*) leaves [43].

TIR1/AFB2 (TRANSPORT INHIBITOR RESPONSE1/AUXIN SIGNALING F-BOX PROTEIN2) Auxin Receptor (TAAR) family F-box proteins are involved in auxin perception and signaling. The expression of *TAAR* is regulated by *miR393* [44]. *MiR393* plays a key role in maintaining proper homeostasis of auxin signaling [45].

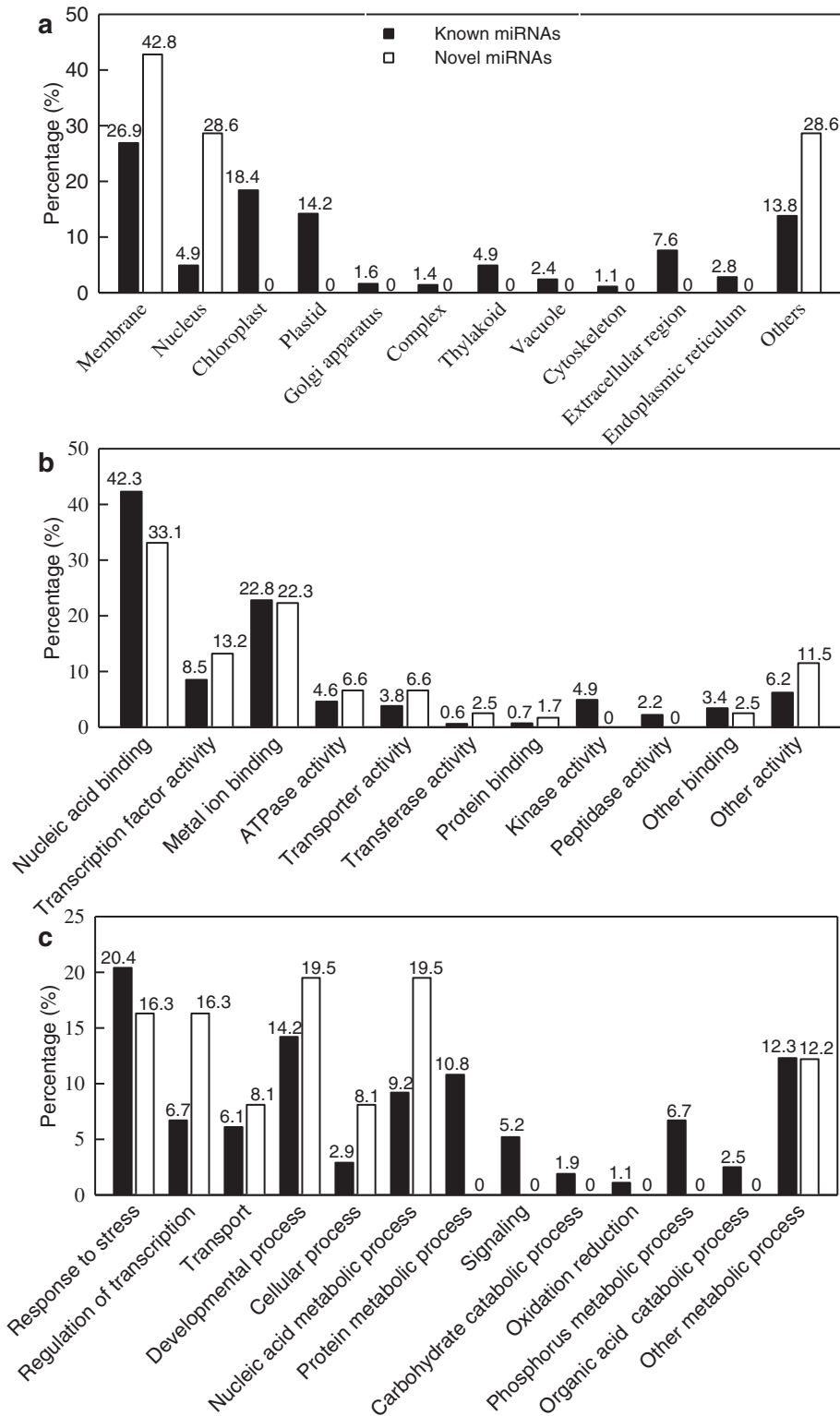


Fig. 3 GO of the predicted target genes for 70 (6) differentially expressed known (novel) miRNAs. Categorization of miRNAs target genes was performed according to cellular component (a), molecular function (b) and biological process (c)

Table 2 qRT-PCR relative expression of experimentally determined or predicted target genes of selected miRNAs

miRNA	Fold change of miRNA	Accession	Homology	Target genes	Relative change of target genes
miR158	-3.35603222**	orange1.1g022993m	AT1G69840.1	SPFH/Band 7/PHB domain-containing membrane-associated protein family	1.9490**
			AT2G03210	Fucosyltransferase 2	1.6482**
miR159	-2.04145817**	orange1.1g001709m	AT3G07400	Lipase class 3 family protein	0.7819*
		orange1.1g039708m	AT5G06100.2	MYB domain protein 33	1.1319*
		orange1.1g044979m	AT4G27330.1	Sporocyteless (SPL)	2.2016**
		orange1.1g046419m	AT4G26930.1	MYB domain protein 97	1.9078**
		orange1.1g011938m	AT3G11440.1	MYB domain protein 65	0.8778**
miR160	1.81653886**	orange1.1g004896m	AT2G28350.1	ARF10	0.7870**
			AT4G30080.1	ARF16	0.7150**
			AT1G77850.1	ARF17	0.9153**
miR164	-2.28320824**	orange1.1g030909m	AT1G56010.2	NAC domain containing protein 1	0.5939**
		orange1.1g047710m	AT5G53950.1	NAC domain transcriptional regulator superfamily protein	1.4205**
		orange1.1g017827m	AT5G61430.1	NAC domain containing protein 100	1.3247**
miR158	-3.35603222**	orange1.1g022993m	AT1G69840.1	SPFH/Band 7/PHB domain-containing membrane-associated protein family	1.9490**
			AT2G03210	Fucosyltransferase 2	1.6482**
miR393	1.66802767**	orange1.1g001709m	AT3G07400	Lipase class 3 family protein	0.7819*
		orange1.1g010049m	AT3G18080.1	B-5 glucosidase 44	0.8384**
		orange1.1g007916m	At3g62980	TIR1	0.7489**
		orange1.1g008325m	At4g03190	AFB1	0.8195**
At3g26810	AFB2		0.7895**		
miR408	-2.55840249**	orange1.1g013075m	At1g12820	AFB3	1.6782**
			At2g30210	Laccase 3	1.5874**
			orange1.1g041358m	At5g05390	Laccase 12
miR477	3.82198862**	orange1.1g048131m	At5g07130	Laccase 13	1.1251*
			At2g02850	Plantacyanin	1.6723**
miR782	-10.08402439**	orange1.1g018483m	AT3G11340.1	UDP-Glycosyltransferase superfamily protein	0.6543**
miR1446	5.01671689**	orange1.1g037028m	HQ202267	MYB transcription factor (MYBML2)	1.5782**
			orange1.1g039969m	NM_001112290	Protein disulfide isomerase (PDIL5-1)
miR1535	1.58529156**	orange1.1g001616m	AT3G63380.1	GRAS family transcription factor family protein	0.7887**
miR2099	10.31417531**	orange1.1g001616m	AT3G63380.1	ATPase E1-E2 type family protein/haloacid dehalogenase-like hydrolase family protein	0.6757**
			AT3G58060.1	Cation efflux family protein	0.7189**
miR2643	-2.52218131**	orange1.1g017694m	AT3G22830.1	Heat shock transcription factor A6B	0.6459**
miR2648	-11.76162602**	orange1.1g018307m	AT1G12500.1	Nucleotide-sugar transporter family protein	0.9924
		orange1.1g020050m	AT5G19890.1	Peroxidase superfamily protein	1.2307**
miR2928	13.58236255**	orange1.1g003798m	AT5G58460.1	Cation/H⁺ exchanger 25	2.0379**
miR2928	13.58236255**	orange1.1g007099m	AT4G04450.1	WRKY family transcription factor	0.4129**
			orange1.1g014735m	AT4G22070.1	WRKY DNA-binding protein 31
		orange1.1g016623m	AT1G62300.1	WRKY family transcription factor	0.5791**

Table 2 qRT-PCR relative expression of experimentally determined or predicted target genes of selected miRNAs (Continued)

miR3446	-1.83050087**	orange1.1g004633m	AT5G66850.1	Mitogen-activated protein kinase kinase kinase 5	1.6310**
		orange1.1g004928m	AT2G25930.1	Hydroxyproline-rich glycoprotein family protein	1.3981**
		orange1.1g036074m	AT4G22200.1	Potassium transport 2/3	1.2999**
miR3946	-1.66667782**	orange1.1g029573m	AT5G47370.1	Homeobox-leucine zipper protein 4 (HB-4)/HD-ZIP protein	0.7342*
		orange1.1g041705m	AT4G25980.1	Peroxidase superfamily protein	1.5621**
		orange1.1g031837m	AT1G08830.1	Copper/zinc superoxide dismutase 1	1.6638**
		orange1.1g016997m	AT1G13310.1	Endosomal targeting BRO1-like domain-containing protein	0.5406**
		orange1.1g014089m	AT1G73390.1	Endosomal targeting BRO1-like domain-containing protein	1.3404**
		orange1.1g027084m	AT3G20560.1	PDI-like 5-3	1.0827*
		orange1.1g017665m	AT3G04070.1	NAC domain containing protein 47	1.6886**
		orange1.1g010076m	AT3G54700.1	Phosphate transporter 1;7	1.7862**
		orange1.1g034408m	AT1G33110.1	MATE efflux family protein	1.5697**
		orange1.1g027612m	AT1G04760.1	Vesicle-associated membrane protein 726	1.2270**
		orange1.1g027026m	AT4G27670.1	Heat shock protein 21	1.3134**
		orange1.1g020124m	AT2G01060.1	MYB-like HTH transcriptional regulator family protein	1.7116**
		orange1.1g011938m	AT3G11440.1	MYB domain protein 65	0.8396**
		orange1.1g005651m	AT1G32640.1	Basic helix-loop-helix (bHLH) DNA-binding family protein	1.3806**
		orange1.1g012387m	AT4G00050.1	Basic helix-loop-helix (bHLH) DNA-binding superfamily protein	1.6480**
orange1.1g004509m	AT2G45290.1	Transketolase	1.1778*		
orange1.1g033760m	AT2G46690.1	SAUR-like auxin-responsive protein family	0.7430**		
miR3953	3.80237602**	orange1.1g016435m	AT5G46590.1	NAC domain containing protein 96	0.7783**
		orange1.1g017142m	AT5G22290.1	NAC domain containing protein 89	1.1842*
miR5037	10.12893993**	orange1.1g013411m	AT2G16980.2	Major facilitator superfamily protein	0.5828**
		orange1.1g016066m	AT2G16990.2	Major facilitator superfamily protein	0.4849**
miR5227	1.8059848**	orange1.1g031467m	AT2G24860.1	DnaJ/Hsp40 cysteine-rich domain superfamily protein	0.4641**
		orange1.1g018585m	AT1G31260.1	Zinc transporter 10 precursor	1.2609**
miR5262	1.64808069**	orange1.1g005832m	AT1G06820.1	Carotenoid isomerase	1.5524**
		orange1.1g003885m	AT5G49890.1	Chloride channel C	0.844**
miR5266	16.22392231**	orange1.1g040022m	AT4G13510.1	Ammonium transporter 1;1	1.2439*
miR5929	-5.83479907**	orange1.1g005910m	AT5G42480.1	Chaperone DnaJ-domain superfamily protein	1.3663**
miR6025	3.39080972**	orange1.1g005832m	AT1G06820.1	Carotenoid isomerase	0.6716
		orange1.1g023118m	AT2G21940.4	Shikimate kinase 1	0.7012**
miR6214	-3.978202**	orange1.1g037661m	AT5G37380.4	Chaperone DnaJ-domain superfamily protein	1.2352**
miR6260	-6.8442483**	orange1.1g010903m	AT5G15130.1	WRKY DNA-binding protein 72	3.2313**
		orange1.1g003752m	AT5G42480.1	Chaperone DnaJ-domain superfamily protein	1.3327**
		orange1.1g041599m	AT1G49330.1	Hydroxyproline-rich glycoprotein family protein	0.9023**
orange1.1g029026m	AT1G64650.1	Major facilitator superfamily protein	1.777**		
miR7539	-4.033976**	orange1.1g002698m	AT2G42600.1	Phosphoenolpyruvate carboxylase 2	1.5943**
		orange1.1g020124m	AT2G01060.1	MYB-like HTH transcriptional regulator family protein	1.1878**
miR7841	-10.61512382**	orange1.1g041450m	AT3G42640.1	H ⁺ -ATPase 8	0.8903**

Both fold change of miRNAs and relative change of target genes are the ratio of B-deficient to -sufficient leaves. The value is an average of at least three biological replicates with three technical replicates; Target genes that had the expected changes in mRNA levels were marked in bold. * and ** indicate a significant difference at $P < 0.05$ and $P < 0.01$, respectively

Table 3 List of differentially expressed miRNAs present in both roots and leaves

MiRNA	Fold change	
	Roots	Leaves
miR418	1.87710209**	2.01596507**
miR4413	3.76410603**	-5.94405631**
miR5037	4.79286276**	10.12893993**
miR3946	5.08067752**	-1.66667782**
miR5259	6.34492626**	-5.83479907**
miR2099	13.49283335**	10.31417531**
miR2622	13.96750818**	10.13868134**
miR2664	14.36084091**	-13.05830635**
miR5266	-1.5614939**	16.22392231**
miR394	-5.15694535**	-1.66667782**
miR3513	-5.84396568**	-7.04650639**
miR5492	-6.7798681**	-5.48597088**
miR5534	-7.1665574**	-2.89672418**
miR5029	-7.43642552**	6.19590225**
miR5211	-8.31439018**	14.53849221**
miR1847	-9.0000212**	10.94295432**
miR158	-10.05808647**	-3.35603222**
miR2921	-10.13114959**	-11.0611889**
miR782	-10.76475548**	-10.08402439**
miR1446	-10.94721705**	5.01671689**
miR5074	-10.94721705**	10.74971862**
miR3443	-11.47199392**	9.96792062**

Data from Additional file 3 and Lu et al. [8]; ** indicates a significant difference at $P < 0.01$

Si-Ammour et al. showed that miR393 down-regulated all four *TAAR* genes by guiding the cleavage of their mRNAs, leading to the changes in auxin perception and some auxin-related leaf development [44]. Stress-induced increase in *miR393* level may decrease the level of *TIR1*, a positive regulator of growth and development, thereby resulting in attenuation in growth and development during stress conditions [14]. Auxin response factors (ARFs) play a role in relaying auxin signaling at the transcriptional level by inducing mainly three groups of genes [i.e., Aux/IAA (Auxin/indole-3-acetic acid), GH3 and small auxin-up RNA (SAUR)] [46, 47]. MiR160 is predicted to target *ARF10*, *ARF16* and *ARF17*. MiR160-directed regulation of *Arabidopsis ARF17* is necessary for the normal growth and development of many organs, proper GH3-like gene expression and perhaps auxin distribution, while the *ARF10* and *ARF16* knockout mutants do not display obvious developmental anomalies [48]. Weakened plant growth and reduced metabolic rate are common survival strategies employed to divert energy and other resources to deal with stress conditions. It has been suggested that the stress-

induced up-regulation of *miR393* and *miR160* might lead to the attenuation of plant growth and development under stress by repressing auxin signaling due to decreased *TIR1* level and by suppressing the ARF-mediated gene expression, respectively, thus promoting plant stress tolerance [47]. Therefore, B-deficiency-induced up-regulation of leaf *miR393* and *miR160* might be an adaptive response of plants to B-deficiency, because the expression of the three genes targeted by miR160 and *TIR1*, *AFB1*, *AFB2* and *AFB3* targeted by miR393 was down-regulated by B-deficiency except for *AFB3* (Table 2). Similarly, the expression of *SAUR-like auxin-responsive protein family* targeted by miR3946 was down-regulated in B-deficient leaves despite decreased expression of *miR3946* (Table 2). By contrast, root *miR3946* was up-regulated by B-deficiency [8].

Leaf *miR164* was down-regulated by B-deficiency (Table 2), as previously observed on transient low nitrate-stressed maize leaves [28]. Water stress led to decreased expression of *miR164* in cassava (*Manihot esculenta*) leaves, while its target gene *MesNAC* (*No Apical Meristem*) was strongly induced [49]. As expected, the expression of *NAC domain transcriptional regulator superfamily protein* and *NAC domain containing protein 100* was induced in B-deficient leaves, while the expression of *NAC domain containing protein 1* was depressed (Table 2). Over-expression of *SNAC1* and *OsNAC6* conferred drought and salt tolerance in rice [50, 51]. *SINAC4-RNAi* tomato plants became less tolerant to salt and drought stress [52]. Therefore, the down-regulation of *miR164* in B-deficient leaves might be involved in the B-deficiency tolerance of plants by improving the expression of *NAC*. However, Xu et al. found that *miR164* was up-regulated in maize leaves under chronic N limitation, and suggested that *miR164* might function in remobilizing the N from old to new leaves to cope with the N-limiting condition via accelerating senescence due to decreased expression of *NAC* [28].

Leaf *miR408* was down-regulated by B-deficiency (Table 2), as previously reported on N-deficient seedlings of *Arabidopsis* [27]. MiR408 targets genes encoding Cu containing proteins such as Cu/Zn SODs (CSDs), plantacyanin and several laccases [23]. Abdel-Ghany and Pilon observed that *miR408* was induced under Cu starvation to down-regulate target gene expression and to save Cu for the most essential functional protein, concluding that might play a role in the regulation of Cu homeostasis [22]. Although B-deficiency decreased leaf concentration of Cu, its level was not lower than the sufficiency range of Cu in citrus leaves [53]. Thus, B-deficiency-induced decrease in *miR408* might be advantageous to plant survival under B-deficiency by regulating Cu homeostasis and improving antioxidant (SOD) activity, because the expression of its four target genes was induced by B-deficiency

except for *laccase 12* (Table 2). Indeed, SOD activity was higher in B-deficient *C. sinensis* leaves than in B-sufficient ones [54]. Also, *SOD* expression was up-regulated in B-deficient *Medicago truncatula* root nodules [55].

Leaf *miR477* was up-regulated by B-deficiency (Table 2), as previously reported on salt-stressed *Populus cathayana* plantlets [56]. NAC and GRAS transcription factors are target genes of *miR477*. NAC is involved in developmental process and stress responses [56], while GRAS proteins play a role in signal transduction and the maintenance and development of meristems [57]. Also, *GRAS* is the target gene of *miR1446* (Table 2), *miR170* and *miR171* [58], and NAC is the target gene of *miR164*, *miR3953* and *miR3946* (Table 2). This indicates the complex regulation in plant development and stress response.

WRKY proteins play important roles in plant responses to (a)biotic stresses, allowing plants to adapt to unfavorable environmental conditions including B-deficiency [59, 60]. Our results showed that leaf transcript of *miR6260* decreased in response to B-deficiency accompanied by increased expression of its target gene: *WRKY DNA-binding protein 72* (Table 2), which agrees with the previous reports that *WRKY3 DNA binding protein* expression was induced in B-deficient *M. truncatula* root nodules [55] and that *WRKY6* was up-regulated in B-deficient *Arabidopsis* roots [60]. Over-expression of various WRKY conferred tolerance to different abiotic stresses in different plant species, possible through the regulation of the reactive oxygen species system [61, 62]. Transgenic *Nicotiana benthamiana* plants over-expressing *GhWRKY39* had enhanced tolerance to salt and oxidative stress and increased expression of genes encoding antioxidant enzymes such as SOD, ascorbate peroxidase (APX), catalase (CAT) and glutathione-S-transferase (GST) [62]. Thus, leaf expression levels of antioxidant enzyme genes might be increased in response to B-deficiency. This agrees with our report that B-deficient citrus leaves had higher activities of SOD, APX, MDAR and GR [54]. Heat shock proteins (HSPs)/chaperones function in protecting plants against various stresses. As expected, the expression of *miR6260* was down-regulated in B-deficient leaves accompanied by increased expression of its one target gene: *chaperone DnaJ-domain superfamily protein* (Table 2). Similarly, leaf expression levels of *miR5929* and *miR6214* were decreased by B-deficiency accompanied by increased expression levels of their corresponding target genes: *DnaJ-domain superfamily protein* (AT5G42480.1 and AT5G37380.4; Table 2). However, the expression of *heat shock transcription factor A6B* targeted by *miR2099* were inhibited in B-deficient leaves despite down-regulated expression of *miR2099* (Table 2). Hydroxyproline-rich glycoproteins (HRGPs) are the most abundant cell wall structural proteins in dicotyledonous plants [63]. Hall and Cannon demonstrated that the cell wall HRGP RSH was required for normal embryo development in

Arabidopsis [64]. Bonilla et al. observed that B-deficiency-induced aberrant cell walls of bean root nodules lacked covalently bound HRGPs [65]. Here, the expression of *HRGP family protein* (AT2G25930.1), a target gene of *miR3446*, was up-regulated in B-deficient leaves (Table 2), thus enhancing plant tolerance to B-deficiency. However, *miR3446* was down-regulated in B-deficient leaves, but its target gene (*HRGP family protein*; AT1G49330.1) was also depressed (Table 2).

B-deficiency lowered leaf expression level of *miR158* (Table 2), as previously obtained on N-deficient *Arabidopsis* seedlings [27] and B-deficient citrus roots [8]. The down-regulation of *miR158* means that its target genes: *SPFH/Band 7/PHB domain-containing membrane-associated protein family, fucosyltransferase 2* and *lipase class 3 family protein* might be up-regulated in B-deficient leaves. However, qRT-PCR showed that the expression of the former two target genes was induced by B-deficiency, while the last one was down-regulated (Table 2). Lu et al. reported that *fucosyltransferase 2* and *lipase class 3 family protein* were down-regulated in B-deficient citrus roots accompanied by decreased expression of *miR158* [8].

The major facilitator superfamily (MFS) is the largest group of transport carriers, which are often coupled to the movement of another ion [66]. Kaya et al. reported that *ATR1*, which encodes a multidrug resistance transport protein of the MFS, was responsible for most of the tolerance of high B in *Saccharomyces cerevisiae*, concluding that *ATR1* was a B exporter [67]. In this study, leaf *miR5037* was induced by B-deficiency accompanied by decreased expression of its target gene: *MFS protein* (Table 2), thus decreasing B export from plants and improving plant tolerance to B-deficiency.

We found that leaf *miR5266* was induced by B-deficiency accompanied by increased expression of its target gene: *ammonium transporter 1;1* (Table 2), which disagrees with our report that the abundance of *miR5266* was lower in B-deficient citrus roots than in controls, while the expression level of *ammonium transporter 1;1* was higher in the former [8].

We observed that *miR3946* was inhibited in B-deficient leaves (Table 2), which disagrees with the previous report that *miR3946* was induced in B-deficient *C. sinensis* roots [8]. All the 17 target genes targeted by *miR3946* were induced by B-deficiency except for *homeobox-leucine zipper protein 4 (HB-4)/HD-ZIP protein, endosomal targeting BRO1-like domain-containing protein* (AT1G13310.1), *MYB domain protein 65* and *SAUR-like auxin-responsive protein family* (Table 2). Previous studies showed that B-deficiency increased the expression levels of some transport-related genes and the abundances of some transport-related proteins in citrus roots [5, 8], thus improving the tolerance of plants to B-deficiency. *BOR1*, an efflux-type B transporter for xylem loading,

play a key role in the tolerance of plants to low B. *Arabidopsis bor1-1* mutant was more sensitive to B-deficiency than the wild type [68]. *Oryza sativa BORI* has been demonstrated to be required for B acquisition by roots and translocation of B into shoots [69]. Thus, B-deficiency-induced up-regulation of leaf *endosomal targeting BRO1-like domain-containing protein* (AT1G73390.1), *phosphate transporter 1;7*, *MATE efflux family protein, vesicle-associated membrane protein 726* (targeted by miR3946), *potassium transport 2/3* (targeted by miR3446), *ammonium transporter 1;1* (targeted by miR5266), *Zn transporter 10 precursor* (targeted by miR5227) and *cation/H⁺ exchanger 25* (targeted by miR2648) involved in cell transport (Table 2) might contribute to the tolerance of citrus to B-deficiency. HD-ZIP transcription factors are found only in plants. The expression of *Hahb-4*, a member of *Helianthus annuus* (sunflower) subfamily I, strongly increased in water-stressed sunflower [70]. Subsequent study showed transgenic *Arabidopsis* plants over-expressing *Hahb-4* were more tolerant to drought by delaying the onset of senescence [71]. Huang et al. demonstrated that *PtrbHLH*, a basic helix-loop-helix transcription factor of *Poncirus trifoliata* might play a crucial role in cold tolerance *via* positively regulating peroxidase (POD)-mediated ROS scavenging [72]. Transketolase is a key enzyme of the pentose phosphate pathway (PPP) in plant cells. Our finding that *transketolase* was up-regulated in B-deficient leaves agrees with the report that transketolase activity in maize moderately increased in response to salt or oxidative stress [73]. In citrus, PPP has been suggested to play a role in the tolerance of plants to B-deficiency by providing reducing power (NADPH) and enhancing the antioxidant capacity [4]. Protein disulfide isomerases (PDIs), which act as molecular chaperones, play a role in the formation of proper disulfide bonds during protein folding [74]. Over-expression of a protein disulfide isomerase-like protein (PDIL) gene conferred Hg tolerance in transgenic plants, which had higher antioxidant capacity and lower levels of superoxide anion radicals, H₂O₂ and malondialdehyde (MDA) [75]. As shown in Table 2, the expression level of *PDIL5-3* targeted by miR3946 was increased in B-deficient leaves. To conclude, down-regulation of *miR3946* in B-deficient leaves might be an adaptive response of plants to B-deficiency.

Carotenoid (Car) isomerase (CRTISO), which catalyzes the isomerization of poly-*cis*-carotenoids to all *trans*-carotenoids in higher plants, is a regulatory step for Car biosynthesis. *Arabidopsis* mutants of *crtiso* had increased accumulation of poly-*cis*-carotenoids and reduced lutein concentration [76, 77]. Here, the expression of *miR6025* was increased and its one target gene: *CRTISO* was decreased in B-deficient leaves (Table 2), thus impairing Car biosynthesis. This agrees with our report that B-

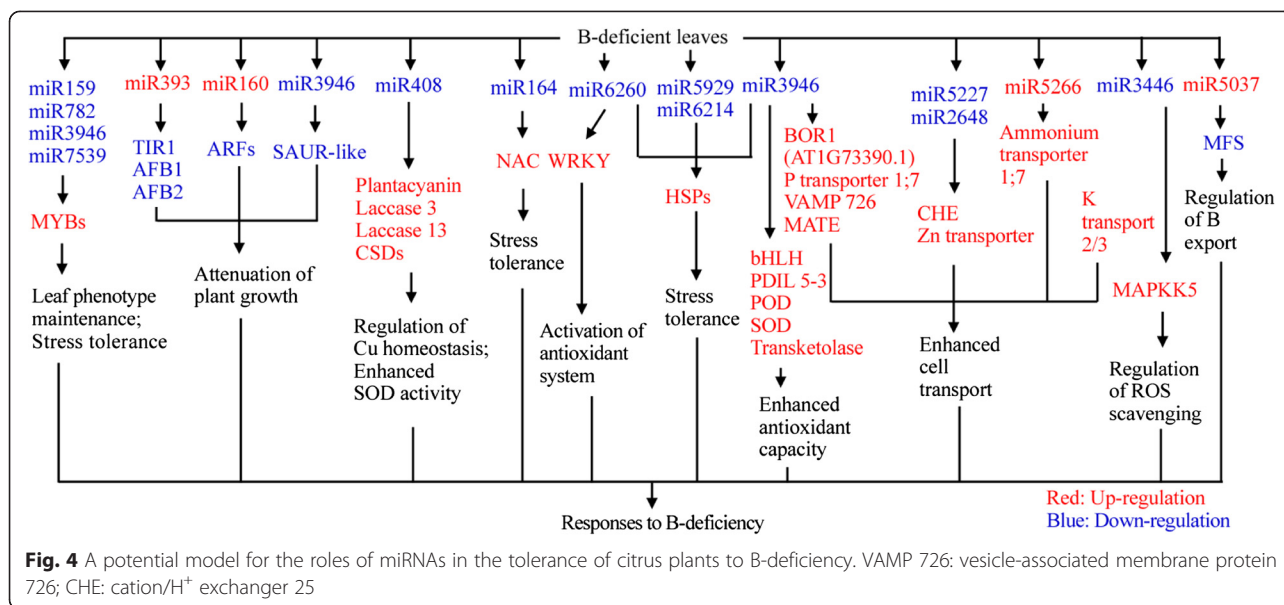
deficient citrus leaves had lower Car concentration [54]. Plant phenolic secondary metabolites and their precursors are synthesized *via* the pathway of shikimate biosynthesis [78]. Shikimate kinase, a key enzyme for the biosynthesis of polyphenols, catalyzes the fifth reaction of the shikimate pathway. As shown in Table 2, the expression level of *shikimate kinase 1* was down-regulated in B-deficient leaves and the expression of *miR6025*, which targets the gene, was up-regulated. This disagrees with our report that B-deficient citrus leaves displayed increased accumulation of phenolics [4].

Mitogen-activated protein kinase (MAPK) cascades play important roles in plant response to various stresses. Each MAPK cascade consists of MAPKs, MAPK kinases (MAPKKs), and MAPKK kinases (MAPKKKs). In plants, MAPKKKs have been shown to be involved in various stresses. Ning et al. showed that transgenic rice plants over-expressing *DSM1* (a putative MAPKKK gene in rice) displayed higher tolerance to dehydration at the seedling stage by regulating ROS scavenging [79]. In this study, leaf transcript of *miR3446* was decreased by B-deficiency and its target gene (*MAPKKK5*) was up-regulated under B-deficiency. This agrees with the report that *MAPKKK* genes were induced by drought, heat, salt, cold, IAA and jasmonic acid (JA) in *Arabidopsis* [80].

Our finding that leaf expression level of *miR7539* decreased in response to B-deficiency, and its target gene (*phosphoenolpyruvate carboxylase, PEPC*) was induced by B-deficiency (Table 2). This agrees with our report that B-deficient citrus leaves had increased activity of PEPC and dark respiration [4].

Conclusion

We identified 734 known and 71 novel miRNAs from B-sufficient and -deficient citrus leaves using Illumina sequencing, and obtained 91 (83 known and 8 novel) up- and 81 (75 known and 6 novel) down-regulated miRNAs from B-deficient citrus leaves. Obviously, the expression of miRNAs was greatly altered in B-deficient leaves, which might play a role in the tolerance of plants to B-deficiency. In this study, we proposed a model for the responses of leaf miRNAs to B-deficiency by integrating the present results with the data available in the previous literatures (Fig. 4). The adaptive responses of leaf miRNAs to B-deficiency might be associated with several aspects: (a) attenuation of plant growth and development by down-regulating *TIR1*, *ARF* and *AFB* due to up-regulated miR393 and miR160, and by lowering the expression of *SAUR-like auxin-responsive protein family* targeted by miR3946, thus enhancing plant stress tolerance; (b) improving the expression of *NACs* due to decreased expression *miR159*, *miR782*, *miR3946* and *miR7539*, hence maintaining leaf phenotype and enhancing the



stress tolerance; (c) activation of the stress responses and antioxidant system due to decreased expression of *miR164*, *miR6260*, *miR5929*, *miR6214*, *miR3946* and *miR3446*; (d) decreased expression of *MFS* resulting from increased expression of *miR5037*, thus lowering B export from plants. In addition, B-deficiency-induced down-regulation of *miR408* might be involved in the tolerance of plants to B-deficiency by regulating Cu homeostasis and enhancing SOD activity. In conclusion, our study reveals some adaptive mechanisms of citrus to B-deficiency.

Methods

Plant culture and B treatments

Both plant culture and B treatments were performed according to Yang et al. [5] and Lu et al. [8]. Briefly, 15-week-old seedlings of 'Xuegan' [*Citrus sinensis* (L.) Osbeck] grown in 6 L pots (two seedlings per pot) containing fine river sand were supplied every other day until dripping with B-deficient (0 μM H₃BO₃) or -sufficient (10 μM H₃BO₃) nutrient solution for 15 weeks. There were 10 replications per B treatment with 2 pots in a completely randomized design. At the end of the experiment, fully-expanded leaves from different replicates and treatments were collected at noon under full sun and frozen immediately in liquid N₂. Leaf samples were stored at -80 °C until extraction. It's worth mentioning that *C. sinensis* is poly-embryonic seed development, an apomictic process in which many embryos are initiated directly from the maternal nucellar cells surrounding the embryo sac containing a developing zygotic embryo [81].

Isolation of leaf sRNAs, library construction and Illumina sequencing

About 0.1 g mixed frozen B-sufficient and -deficient leaves from five replications were used to extract RNA. Total RNA was extracted from frozen leaves using TRIzol reagent (Invitrogen, Carlsbad, CA) following manufacturer's instructions. Two sRNA libraries were constructed according to Lu et al. [8]. High throughput sequencing was performed on a Solexa sequencer (Illumina) at the Beijing Genomics Institute (BGI), Shenzhen, China.

sRNA annotation and miRNA identification

Both sRNA annotation and miRNA identification were performed according to Lu et al. [8]. Briefly, software developed by the BGI was used to deal with the raw data from the Solexa sequencing. Clean reads were then used to analyze length distribution and common/specific sequences. Thereafter, the clear reads were mapped to *C. sinensis* genome (JGIversion 1.1, http://phytozome.jgi-doe.gov/pz/portal.html#linfo?alias=Org_Csinensis) using SOAP, only perfectly mapped sequences were retained and analyzed further. rRNAs, tRNAs, snRNAs and snoRNAs were removed from the sRNAs sequences through BLASTn search using NCBI Genebank database (<http://www.ncbi.nlm.nih.gov/blast/Blast.cgi/>) and Rfam (12.0) database (<http://www.sanger.ac.uk/resources/databases/rfam.html>) ($e = 0.01$). The remaining sequences were aligned with known plant miRNAs from miRBase 21 (<http://www.mirbase.org/>). Only the perfectly matched sequences were considered to be conserved miRNAs. Reads that were not annotated were used to predict novel miRNAs using a prediction software Mireap (

sourceforge.net/projects/mireap/), which was developed by the BGI, by exploring the secondary structure, the Dicer cleavage site and the minimum free energy of the unannotated small RNA tags which could be mapped to genome. In addition, we used MTide: an integrated tool for the identification of miRNA-target interaction in plants (<http://bis.zju.edu.cn/MTide>) [82] and DNAMAN 8 (<http://www.lynonn.com/pc/framepc.html>) to predict novel miRNA. Only these miRNA candidates that were simultaneously predicted by the three softwares were considered to be real novel miRNAs.

Differential expression analysis of miRNAs

Both the fold change between B-deficiency and -sufficiency and the *P*-value were calculated from the normalized expression of TPM [83]. A 1.5 log₂-fold cut-off was set to determine up- and down-regulated miRNAs in addition to a *P*-value of less than 0.01 [8].

Target prediction of miRNAs

This was performed by RNAhybrid based on rules suggested by Allen et al. [84] and Schwab et al. [85].

Functions of the potential targets of the differentially expressed miRNAs

All targets of the differentially expressed miRNAs were mapped to GO terms in the database (<http://www.geneontology.org/>), and calculated gene numbers for each term. The GO results were expressed as three categories: cellular component, molecular function, biological process [8].

Validation of miRNA expression by stem-loop qRT-PCR

The detection of miRNA expression was performed using stem-loop qRT-PCR method, stem-loop primers for reverse transcription and primers for qRT-PCR were listed in Additional file 8. Total RNA was reverse-transcribed using Taqman[®] MicroRNA Reverse Transcription Kit (USA), and SYBR[®] Premix Ex Taq[™] II (Takara, Japan) kit was used for qRT-PCR. MiRNA special (forward) primers were designed according to the miRNA sequence but excluded the last six nucleotides at 3' end of the miRNA. A 5' extension of several nucleotides, which was chosen randomly and relatively GC-rich, was added to each forward primer to increase the melting temperature [86]. All the primers were assigned to Primer Software Version 5.0 (PREMIER Biosoft International, USA) to assess their quality. For qRT-PCR, 20 μL reaction solution contained 10 μL ready-to-use SYBR[®] Premix Ex Taq[™] II (Takara, Japan), 0.8 μL 10 μM miRNA forward primer, 0.8 μL 10 μM Uni-miR qPCR primer, 2 μL cDNA template and 6.4 μL dH₂O. The cycling conditions were 60 s at 95 °C, followed by 40 cycles of 95 °C for 10 s, 60 °C for 30 s. qRT-PCR was performed on the ABI 7500 Real Time System. Samples

for qRT-PCR were run in at least three biological replicates with two technical replicates. Relative miRNA expression was calculated using ddCt algorithm. For the normalization of miRNA expression, *actin* (AEK97331.1) was used as an internal standard and the leaves from control plants were used as reference sample, which was set to 1.

qRT-PCR analysis of miRNA target gene expression

Total RNA was extracted from frozen B-sufficient and -deficient leaves using TRIzol reagent (Invitrogen, Carlsbad, CA) following manufacturer's instructions. The sequences of the F and R primers used were given in Additional file 9. qRT-PCR analysis of miRNA target gene expression was performed using a ABI 7500 Real Time System according to Lu et al. [8].

Experimental design and statistical analysis

There were 20 pot seedlings per treatment in a completely randomized design. Experiments were performed with 3 replicates. Differences among treatments were separated by the least significant difference (LSD) test at *P* < 0.05 level.

Availability of data and materials

"The data set supporting the results of this article are available in the Gene Expression Omnibus repository under accession no GSE72108 (<http://www.ncbi.nlm.nih.gov/geo/query/acc.cgi?acc=GSE72108>)". The mature miRNA and precursor sequences will be submitted to miRBase registry and assigned final names after final acceptance of the manuscript.

Additional files

Additional file 1: Length distribution of small RNAs from control and B-deficient leaves of *Citrus sinensis* seedlings. (DOC 81 kb)

Additional file 2: List of known miRNAs in *Citrus sinensis* leaves. (DOC 1525 kb)

Additional file 3: List of known miRNAs in *Citrus sinensis* leaves after removing these miRNAs with normalized read-count less than 10 TPM in the two miRNA libraries constructed from control and B-deficient leaves. (DOC 452 kb)

Additional file 4: List of novel miRNAs in *Citrus sinensis* leaves. (DOC 158 kb)

Additional file 5: List of novel miRNAs in *Citrus sinensis* leaves after removing these miRNAs with normalized read-count less than 10 TPM in two miRNA libraries constructed from control and B-deficient leaves. (DOC 69 kb)

Additional file 6: List of target genes for parts of known miRNAs in *Citrus sinensis* leaves. (DOC 198 kb)

Additional file 7: List of target genes for parts of novel miRNAs in *Citrus sinensis* leaves. (DOC 33 kb)

Additional file 8: List of stem loop qRT-PCR primers. (DOC 61 kb)

Additional file 9: Specific primer pairs used for qRT-PCR expression analysis of selected miRNA target genes. (DOC 160 kb)

Competing interests

The authors declare that they have no competing interests.

Authors' contributions

YBL carried out most of the experiments and drafted the manuscript; YPQ participated in the design of the study. LTY participated in the design of the study and coordination; PG participated in data analysis; YL directed the study; LSC designed and directed the study and revised the manuscript.

Acknowledgments

This study was jointly supported by the National Natural Science Foundation of China (No. 31171947) and the earmarked fund for China Agriculture Research System (No. CARS-27).

Author details

¹College of Resource and Environmental Science, Fujian Agriculture and Forestry University, Fuzhou 350002, China. ²Institute of Horticultural Plant Physiology, Biochemistry and Molecular Biology, Fujian Agriculture and Forestry University, Fuzhou 350002, China. ³Institute of Materia Medica, Fujian Academy of Medical Sciences, Fuzhou 350001, China. ⁴The Higher Educational Key Laboratory of Fujian Province for Soil Ecosystem Health and Regulation, Fujian Agriculture and Forestry University, Fuzhou 350002, China. ⁵Fujian Key Laboratory for Plant Molecular and Cell Biology, Fujian Agriculture and Forestry University, Fuzhou 350002, China.

Received: 6 June 2015 Accepted: 8 October 2015

Published online: 04 November 2015

References

- Cakmak I, Römheld V. Boron deficiency-induced impairments of cellular functions in plants. *Plant Soil*. 1997;193:71–83.
- Dell B, Huang L. Physiological response of plants to low boron. *Plant Soil*. 1997;193:103–20.
- Chen LS, Han S, Qi YP, Yang LT. Boron stresses and tolerance in citrus. *Afr J Biotech*. 2012;11:5961–9.
- Lu YB, Yang LT, Li Y, Xu J, Liao TT, Chen YB, et al. Effects of boron deficiency on major metabolites, key enzymes and gas exchange in leaves and roots of *Citrus sinensis* seedlings. *Tree Physiol*. 2014;34:608–18.
- Yang LT, Qi YP, Lu YB, Guo P, Sang W, Feng H, et al. iTRAQ protein profile analysis of *Citrus sinensis* roots in response to long-term boron-deficiency. *J Proteomics*. 2013;93:179–206.
- Huang YZ, Li J, Wu SH, Pang DM. Nutrition condition of the orchards in the main production areas of Guanxihoney pomelo trees (Pinhe county). *J Fujian Agri Univ*. 2001;30:40–3.
- Jones-Rhoades MW, Bartel DP, Bartel B. MicroRNAs and their regulatory roles in plants. *Annu Rev Plant Biol*. 2006;57:19–53.
- Lu YB, Yang LT, Qi YP, Li Y, Li Z, Chen YB, et al. Identification of boron-deficiency-responsive microRNAs in *Citrus sinensis* roots by Illumina sequencing. *BMC Plant Biol*. 2014;14:123.
- Paul S, Datta SK, Datta K. MiRNA regulation of nutrient homeostasis in plants. *Front Plant Sci*. 2015;6:232.
- Zeng H, Wang G, Hu X, Wang H, Du L, Zhu Y. Role of microRNAs in plant responses to nutrient stress. *Plant Soil*. 2014;374:1005–21.
- Chiou TJ, Lin SI. Signaling network in sensing phosphate availability in plants. *Annu Rev Plant Biol*. 2011;62:185–206.
- Xu F, Liu Q, Chen L, Kuang J, Walk T, Wang J, et al. Genome-wide identification of soybean microRNAs and their targets reveals their organ-specificity and responses to phosphate starvation. *BMC Genomics*. 2013;14:66.
- Hsieh LC, Lin SI, Shih ACC, Chen JW, Lin WY, Tseng CY, et al. Uncovering small RNA-mediated responses to phosphate deficiency in *Arabidopsis* by deep sequencing. *Plant Physiol*. 2009;151:2120–32.
- Shukla LI, Chinnusamy V, Sunkar R. The role of microRNAs and other endogenous small RNAs in plant stress responses. *Biochim Biophys Acta*. 1779;2008:743–8.
- Hackenberg M, Huang PJ, Huang CY, Shi BJ, Gustafson P, Langridge P. A comprehensive expression profile of microRNAs and other classes of non-coding small RNAs in barley under phosphorous-deficient and -sufficient conditions. *DNA Res*. 2013;20:109–25.
- Zhu YY, Zeng HQ, Dong CX, Yin XM, Shen QR, Yang ZM. MicroRNA expression profiles associated with phosphorus deficiency in white lupin (*Lupinus albus* L.). *Plant Sci*. 2010;178:23–9.
- Valdés-López O, Yang SS, Aparicio-Fabre R, Graham PH, Reyes JL, Vance CP, et al. MicroRNA expression profile in common bean (*Phaseolus vulgaris*) under nutrient deficiency stresses and manganese toxicity. *New Phytol*. 2010;187:805–18.
- Pant BD, Musialak-Lange M, Nuc P, May P, Buhtz A, Kehr J, et al. Identification of nutrient responsive *Arabidopsis* and rapeseed microRNAs by comprehensive real-time polymerase chain reaction profiling and small RNA sequencing. *Plant Physiol*. 2009;150:1541–55.
- Gu M, Xu K, Chen AQ, Zhu YY, Tang GL, Xu GH. Expression analysis suggests potential roles of microRNAs for phosphate and arbuscular mycorrhizal signaling in *Solanum lycopersicum*. *Physiol Plant*. 2010;138:226–37.
- Pei L, Jin Z, Li K, Yin H, Wang J, Yang A. Identification and comparative analysis of low phosphate tolerance associated microRNAs in two maize genotypes. *Plant Physiol Biochem*. 2013;70:221–34.
- Zhao X, Liu X, Guo C, Gu J, Xiao K. Identification and characterization of microRNAs from wheat (*Triticum aestivum* L.) under phosphorus deprivation. *J Plant Biochem Biotechnol*. 2013;22:113–23.
- Abdel-Ghany SE, Pilon M. MicroRNA-mediated systemic down-regulation of copper protein expression in response to low copper availability in *Arabidopsis*. *J Biol Chem*. 2008;283:15932–45.
- Yamasaki H, Abdel-Ghany SE, Cohu CM, Kobayashi Y, Shikanai T, Pilon M. Regulation of copper homeostasis by microRNA in *Arabidopsis*. *J Biol Chem*. 2007;282:16369–78.
- Liang G, Yang F, Yu D. MicroRNA395 mediates regulation of sulfate accumulation and allocation in *Arabidopsis thaliana*. *Plant J*. 2010;62:1046–57.
- Kong WW, Yang ZM. Identification of iron-deficiency responsive microRNA genes and cis-elements in *Arabidopsis*. *Plant Physiol Biochem*. 2010;48:153–9.
- Waters BM, McInturf SA, Stein RJ. Rosette iron deficiency transcript and microRNA profiling reveals links between copper and iron homeostasis in *Arabidopsis thaliana*. *J Exp Bot*. 2012;63:5903–18.
- Liang G, He H, Yu D. Identification of nitrogen starvation-responsive microRNAs in *Arabidopsis thaliana*. *PLoS One*. 2012;7:e48951.
- Xu Z, Zhong S, Li X, Li W, Rothstein SJ, Zhang S, et al. Genome-wide identification of microRNAs in response to low nitrate availability in maize leaves and roots. *PLoS One*. 2011;6:e28009.
- Zhao M, Ding H, Zhu JK, Zhang F, Li WX. Involvement of miR169 in the nitrogen-starvation responses in *Arabidopsis*. *New Phytol*. 2011;190:906–15.
- Lu Y, Qi Y, Lee J, Guo P, Ye X, Jia M, et al. Long-term boron-deficiency-responsive genes revealed by cDNA-AFLP differ between *Citrus sinensis* roots and leaves. *Front Plant Sci*. 2015;6:585.
- Chapman HD. The mineral nutrition of citrus. In: Reuther W, Webber HJ, Batchelor LD, editors. The citrus industry, volume 2. CA: Division of Agricultural Sciences, University of California; 1968. p. 127–89.
- Li R, Li Y, Kristiansen K, Wang J. SOAP: short oligonucleotide alignment program. *Bioinformatics*. 2008;24:713–4.
- Xu Q, Liu Y, Zhu A, Wu X, Ye J, Yu K, et al. Discovery and comparative profiling of microRNAs in a sweet orange red-flesh mutant and its wild type. *BMC Genomics*. 2010;11:246.
- Song C, Wang C, Zhang C, Korir NK, Yu H, Ma Z, et al. Deep sequencing discovery of novel and conserved microRNAs in trifoliolate orange (*Citrus trifoliata*). *BMC Genomics*. 2010;11:431.
- Chen L, Wang T, Zhao M, Tian Q, Zhang WH. Identification of aluminum-responsive microRNAs in *Medicago truncatula* by genome-wide high-throughput sequencing. *Planta*. 2012;235:375–86.
- Meyers BC, Axtell MJ, Bartel B, Bartel DP, Baulcombe D, Bowman JL, et al. Criteria for annotation of plant microRNAs. *Plant Cell*. 2008;20:3186–90.
- Zhao M, Tai H, Sun S, Zhang F, Xu Y, Li WX. Cloning and characterization of maize miRNAs involved in responses to nitrogen deficiency. *PLoS One*. 2012;7:e29669.
- Patade VY, Suprasanna P. Short-term salt and PEG stresses regulate expression of microRNA, miR159 in sugarcane leaves. *J Crop Sci Biotech*. 2010;13:177–82.
- Zeng HQ, Zhu YY, Huang SQ, Yang ZM. Analysis of phosphorus-deficient responsive miRNAs and cis-elements from soybean (*Glycine max* L.). *J Plant Physiol*. 2010;167:1289–97.
- Palatnik J, Allen E, Wu X, Schommer C, Schwab R, Carrington J, et al. Control of leaf morphogenesis by microRNAs. *Nature*. 2003;425:257–63.
- Dai X, Xu Y, Ma Q, Xu W, Wang T, Xue Y, et al. Overexpression of an R1R2R3 MYB gene, *OsMYB3R-2*, increases tolerance to freezing, drought, and salt stress in transgenic *Arabidopsis*. *Plant Physiol*. 2007;143:1739–51.
- Wimmer MA, Eichert T. Review: mechanisms for boron deficiency-mediated changes in plant water relations. *Plant Sci*. 2013;203–204:25–32.

43. Yang CQ, Liu YZ, An JC, Li S, Jin LF, Zhou GF, et al. Digital gene expression analysis of corky split vein caused by boron deficiency in 'Newhall' navel orange (*Citrus sinensis* Osbeck) for selecting differentially expressed genes related to vascular hypertrophy. *PLoS One*. 2013;8:e65737.
44. Si-Ammour A, Windels D, Arn-Boulidoires E, Kutter C, Ailhas J, Meins Jr F, et al. MIR393 and secondary siRNAs regulate expression of the TIR1/AFB2 auxin receptor clade and auxin-related development of *Arabidopsis* leaves. *Plant Physiol*. 2010;157:683–91.
45. Windels D, Vazquez F. MIR393: integrator of environmental cues in auxin signaling? *Plant Signal Behav*. 2011;6:1672–75.
46. Chapman EJ, Estelle M. Mechanism of auxin-regulated gene expression in plants. *Annu Rev Genet*. 2009;43:265–85.
47. Sunkar R, Li YF, Jagadeeswaran G. Functions of microRNAs in plant stress. *Trends Plant Sci*. 2012;17:196–203.
48. Mallory AC, Bartel DP, Bartel B. MicroRNA-directed regulation of *Arabidopsis AUXIN RESPONSE FACTOR17* is essential for proper development and modulates expression of early auxin response genes. *Plant Cell*. 2005;17:1360–75.
49. Phookaew P, Netrphan S, Sojikul P, Narangajavana J. Involvement of miR164- and miR167-mediated target gene expressions in responses to water deficit in cassava. *Biol Plant*. 2014;58:469–78.
50. Hu H, Dai M, Yao J, Xiao B, Li X, Zhang Q, et al. Overexpressing a NAM, ATAF, and CUC (NAC) transcription factor enhances drought resistance and salt tolerance in rice. *Proc Natl Acad Sci U S A*. 2006;103:12987–92.
51. Nakashima K, Tran LS, Nguyen DV, Fujita M, Maruyama K, Todaka D, et al. Functional analysis of a NAC-type transcription factor OsNAC6 involved in abiotic and biotic stress responsive gene expression in rice. *Plant J*. 2007;51:617–30.
52. Zhu M, Chen G, Zhang J, Zhang Y, Xie Q, Zhao Z, et al. The abiotic stress-responsive NAC-type transcription factor SINAC4 regulates salt and drought tolerance and stress-related genes in tomato (*Solanum lycopersicum*). *Plant Cell Rep*. 2014;33:1851–63.
53. Zhuang YM. Citrus nutrition and fertilization. Beijing: China Agriculture Press; 1994.
54. Han S, Chen LS, Jiang HX, Smith BR, Yang LT, Xie CY. Boron deficiency decreases growth and photosynthesis, and increases starch and hexoses in leaves of citrus seedlings. *J Plant Physiol*. 2008;165:1331–41.
55. Redondo-Nieto M, Maunoury N, Mergaert P, Kondorosi E, Bonilla I, Bolaños L. Boron and calcium induce major changes in gene expression during legume nodule organogenesis. Does boron have a role in signalling? *New Phytol*. 2012;195:14–9.
56. Zhou J, Liu M, Jiang J, Qiao G, Lin S, Li H, et al. Expression profile of miRNAs in *Populus cathayana* L. and *Salix matsudana* Koidz under salt stress. *Mol Biol Rep*. 2012;39:8645–54.
57. Bolle C. The role of GRAS proteins in plant signal transduction and development. *Planta*. 2004;218:683–92.
58. Rhoades MW, Reinhart BJ, Lim LP, Burge CB, Bartel B, Bartel DP. Prediction of plant microRNA targets. *Cell*. 2002;110:513–20.
59. Pan LJ, Jiang L. Identification and expression of the WRKY transcription factors of *Carica papaya* in response to abiotic and biotic stresses. *Mol Biol Rep*. 2014;41:1215–25.
60. Kasajima I, Ide Y, Yokota Hirai M, Fujiwara T. WRKY6 is involved in the response to boron deficiency in *Arabidopsis thaliana*. *Physiol Plant*. 2010;139:80–92.
61. Liu QL, Xu KD, Pan YZ, Jiang BB, Liu GL, Jia Y, et al. Functional analysis of a novel chrysanthemum *WRKY* transcription factor gene involved in salt tolerance. *Plant Mol Biol Rep*. 2014;32:282–9.
62. Shi W, Liu D, Hao L, Wu C, Guo X, Li H. GhWRKY39, a member of the WRKY transcription factor family in cotton, has a positive role in disease resistance and salt stress tolerance. *Plant Cell Tiss Org*. 2014;118:17–32.
63. Sommer-Knudsen J, Bacic A, Clarke AE. Hydroxyproline-rich plant glycoproteins. *Phytochemistry*. 1997;47:483–97.
64. Hall Q, Cannon MC. The cell wall hydroxyproline-rich glycoprotein RSH is essential for normal embryo development in *Arabidopsis*. *Plant Cell*. 2002;14:1161–72.
65. Bonilla I, Mergold-Villaseñor C, Campos ME, Sánchez N, Pérez H, López L, et al. The aberrant cell walls of boron-deficient bean root nodules have no covalently bound hydroxyproline-/proline-rich proteins. *Plant Physiol*. 1997;115:1329–40.
66. Lin Si, Santi C, Jobet E, Lacut E, El Kholti N, Karlowski WM, et al. Complex regulation of two target genes encoding SPX-MFS proteins by rice miR827 in response to phosphate starvation. *Plant Cell Physiol*. 2010;51:2119–31.
67. Kaya A, Karakaya HC, Fomenko DE, Gladyshev VN, Koc A. Identification of a novel system for boron transport: Atr1 is a main boron exporter in yeast. *Mol Cell Biol*. 2009;29:3665–74.
68. Takano J, Noguchi K, Yasumori M, Kobayashi M, Gajdos Z, Miwa K, et al. *Arabidopsis* boron transporter for xylem loading. *Nature*. 2002;420:337–40.
69. Nakagawa Y, Hanaoka H, Kobayashi M, Miyoshi K, Miwa K, Fujiwara T. Cell-type specificity of the expression of Os *BOR1*, a rice efflux boron transporter gene, is regulated in response to boron availability for efficient boron uptake and xylem loading. *Plant Cell*. 2007;19:2624–35.
70. Gago GM, Almoguera C, Jordano J, Gonzalez DH, Chan RL. *Habb-4*, a homeobox-leucine zipper gene potentially involved in abscisic acid-dependent responses to water stress in sunflower. *Plant Cell Environ*. 2002;25:633–40.
71. Dezar CA, Gago GM, Gonzalez DH, Chan RL. *Habb-4*, a sunflower homeobox-leucine zipper gene, is a developmental regulator and confers drought tolerance to *Arabidopsis thaliana* plants. *Transgenic Res*. 2005;14:429–40.
72. Huang XS, Wang W, Zhang Q, Liu JH. A basic helix-loop-helix transcription factor, PtrbHLH, of *Poncirus trifoliata* confers cold tolerance and modulates peroxidase-mediated scavenging of hydrogen peroxide. *Plant Physiol*. 2013;162:1178–94.
73. Rapala-Kozik M, Kowalska E, Ostrowska K. Modulation of thiamine metabolism in *Zea mays* seedlings under conditions of abiotic stress. *J Exp Bot*. 2008;59:4133–43.
74. Houston NL, Fan C, Xiang JQ, Schulze JM, Jung R, Boston RS. Phylogenetic analyses identify 10 classes of the protein disulfide isomerase family in plants, including single-domain protein disulfide isomerase-related proteins. *Plant Physiol*. 2005;137:762–78.
75. Chen Z, Pan Y, Wang S, Ding Y, Yang W, Zhu C. Overexpression of a protein disulfide isomerase-like protein from *Methanothermobacter thermoautotrophicum* enhances mercury tolerance in transgenic rice. *Plant Sci*. 2012;197:10–20.
76. Cazzonelli CI, Roberts AC, Carmody ME, Pogson BJ. Transcriptional control of SET DOMAIN GROUP 8 and CAROTENOID ISOMERASE during *Arabidopsis* development. *Mol Plant*. 2010;3:174–91.
77. Wei J, Xu M, Zhang D, Mi H. The role of carotenoid isomerase in maintenance of photosynthetic oxygen evolution in rice plant. *Acta Biochim Biophys Sin*. 2010;42:457–63.
78. Tohge T, Watanabe M, Hoefgen R, Fernie AR. The evolution of phenylpropanoid metabolism in the green lineage. *Crit Rev Biochem Mol Biol*. 2013;48:123–52.
79. Ning J, Li X, Hicks LM, Xiong L. A Raf-like MAPKKK gene DSM1 mediates drought resistance through reactive oxygen species scavenging in rice. *Plant Physiol*. 2010;152:876–90.
80. Wu J, Wang J, Pan C, Guan X, Wang Y, Liu S, et al. Genome-wide identification of MAPKK and MAPKKK gene families in tomato and transcriptional profiling analysis during development and stress response. *PLoS One*. 2014;9:e103032.
81. Aleza P, Juárez J, Ollitrault P, Navarro L. Polyembryony in non-apomictic citrus genotypes. *Ann Bot*. 2010;106:533–45.
82. Zhang Z, Jiang L, Wang J, Gu P, Chen M. MTide: an integrated tool for the identification of miRNA-target interaction in plants. *Bioinformatics*. 2015;31(2):290–1.
83. Wang T, Chen L, Zhao M, Tian Q, Zhang WH. Identification of drought-responsive microRNAs in *Medicago truncatula* by genome-wide high throughput sequencing. *BMC Genomics*. 2011;12:367.
84. Allen E, Xie Z, Gustafson AM, Carrington JC. MicroRNA-directed phasing during trans-acting siRNA biogenesis in plants. *Cell*. 2005;121:207–21.
85. Schwab R, Palatnik JF, Riester M, Schommer C, Schmid M, Weigel D. Specific effects of microRNAs on the plant transcriptome. *Dev Cell*. 2005;8:517–27.
86. Chen C, Ridzon DA, Broomer AJ, Zhou Z, Lee DH, Nguyen JT, et al. Real-time quantification of microRNAs by stem-loop RT-PCR. *Nucleic Acids Res*. 2005;33:e179.